IMPROVING ECO-SUSTAINABLE CHARACTERISTICS AND ENERGY EFFICIENCY OF EVAPORATIVE FLUID COOLER VIA EXPERIMENTAL AND NUMERICAL STUDY

by

Predrag O. RAŠKOVIĆ, Goran D. VUČKOVIĆ, and Mića V. VUKIĆ

Original scientific paper
UDC: 66.045.5:519.876.5
BIBLID: 0354-9836, *12* (2008), 4, 89-103
DOI: 10.2298/TSCI0804089R

This paper presents an on-going research project that aims to identify possibilities for wider use of evaporative cooling in process industry, especially the use of evaporative fluid cooler units. Experimental study is performed on small scale evaporative fluid cooler, while the correlation based model has been carried out to explore the detailed heat and mass transfer processes inside this unit. Numerical integration of mathematical model is executed by new approach, based on differential, collocation Simpson method. Proposed models have been verified by comparing the computed results with those obtained by the experimental measurements. The results of research will enable the creation of more comprehensive simulation software, with wider range of operating and construction parameters.

Key words: *evaporative fluid cooler, experimental study, numerical integration, Simpson method, simulation software*

Introduction

During the past few decades a significant increase in energy and water consumption has been produced due to the growth in cooling demand. In order to response on this challenge it become necessary to develop new low energy cooling technologies (LECT), which have better eco-sustainable characteristics and less life-cycle cost than comparable refrigeration systems. Life-cycle cost includes all money values such as first cost, energy, water, time value of money, and maintenance costs.

One of the base principle for accomplishing the LECT, evaporative cooling (EC), is a physical phenomenon in which evaporation of a liquid, typically into surrounding air, cools an object or a liquid in contact with it. EC does not contribute to ozone depletion or global warming since it enabled the use of low quality sources of cooling (like ambient air, ground water or, in some cases, the lower quality water). The energy savings of EC translates into reduced energy consumption and decrease the peak electricity demand load, especially during summer cooling hours.

The cooling effect of EC can be applied directly to the evaporative cooled heat exchangers (ECHE). These process units are used in many applications such as power plants, air-conditioning, and refrigeration, mainly because their relatively low price and easy maintains. The family of ECHE is usually considered under the applications of closed wet cooling towers (CWCT), evaporative fluid coolers (EFC), and evaporative condensers (ECN). The difference among them is primary based on the kind of process and desired temperature of the fluid to be cooled (*e. g.* the ECN condenses a refrigerant in gaseous form to liquid, while a CWCT simply cools down water, EFC usually operate at higher temperature levels than CWCT, ...). However, the principle of operation is similar in all cases.

This paper presents an on-going research project that aims to identify possibilities for wider use of evaporative cooling in process industry, especially the EFC units. For that purpose a small scale EFC plant was built in the Laboratory of Thermal Department of Mechanical Engineering Faculty on University of Niš, Serbia. Scale modeling approach is chosen mainly because two reasons. First, experimental approaches carried out for a real size EFC would be costly and time consuming; second, it would be very difficult to obtain an accurate measurement of the fluids distribution and flow resistance within such unit. Thermal analysis of EFC is realized by correlation based model, developed by Zalewski *et al.* [1, 2]. Numerical integration of model is executed by application of differential, collocation Simpson's method, and translated in simulation software for bare-tube EFC performances. This kind of integration presents a new solution approach according to the literature review. The results of simulation are compared with the results obtained from the experimental measurements, performed on a small scale EFC plant. Reasonable agreement will enable the creation of new simulation software which will amplify the range of air and water input parameters as well the use of the equipment with different physical performances.

Principle of EFC operation

The phenomenon of cooling by evaporation in the conventional EFC has long been recognized as the logical development of the cooling tower/heat exchanger combination. Operation principle and design theories of the EFC is very similar to the open cooling tower (OCT) with one exception, the process fluid being cooled is not directly exposed to the atmosphere air or the external water. Because of that, EFC may be regarded as a cooling tower in which the packing is replaced by a bank of tubes, carrying the process fluid. Another difference between OCT and EFC is based on their thermal performances. In the case of OCT the packing temperature is usually assumed to be constant, whereas the temperature of the fluid in the tubes (and hence the tube surface temperature) vary in the case of EFC. Thus, the design models for the EFC are more complicated than those for the conventional cooling tower.

The main advantage of EFC compared with an OCT is the low contamination risks caused by airborne dusts and corrosion, since the process fluid never contacts the outside air and external water. The main drawback of EFC is the increase of cost and the size because a larger heat-exchange surface is required to reach the same heat transfer as in OCT. In order to reduce water consumption, some EFC can operate in a dry regime when the outdoor conditions are favorable and the cooling demand is low. In this case the temperature oh heat sink is higher, decrease in heat transfer rate is considerable and as a result, the efficiency of cooling becomes much lower. When compared with dry regime, conventional EFC can achieve lower temperatures and cool the process fluid close to the wet bulb temperature of the air. Its main weakness is its vulnerability to fouling inside the tubes, especially in the case when the temperature of process fluid rises above 50 °C. This often limits the process side temperature to less than 80 °C.

Conventional EFC can be presented as the three-fluid exchanger in which process fluid, spray water, and air flowed (usually in different directions) and interact whit each other (fig. 1a). Inside the EFC exists two separate liquid fluid circuits: (1) an external circuit, in which external (spray) water circulates over the tubes and mixes with the outside air, and (2) an internal circuit, in which the process fluid (commonly hot water) circulates inside the tubes.

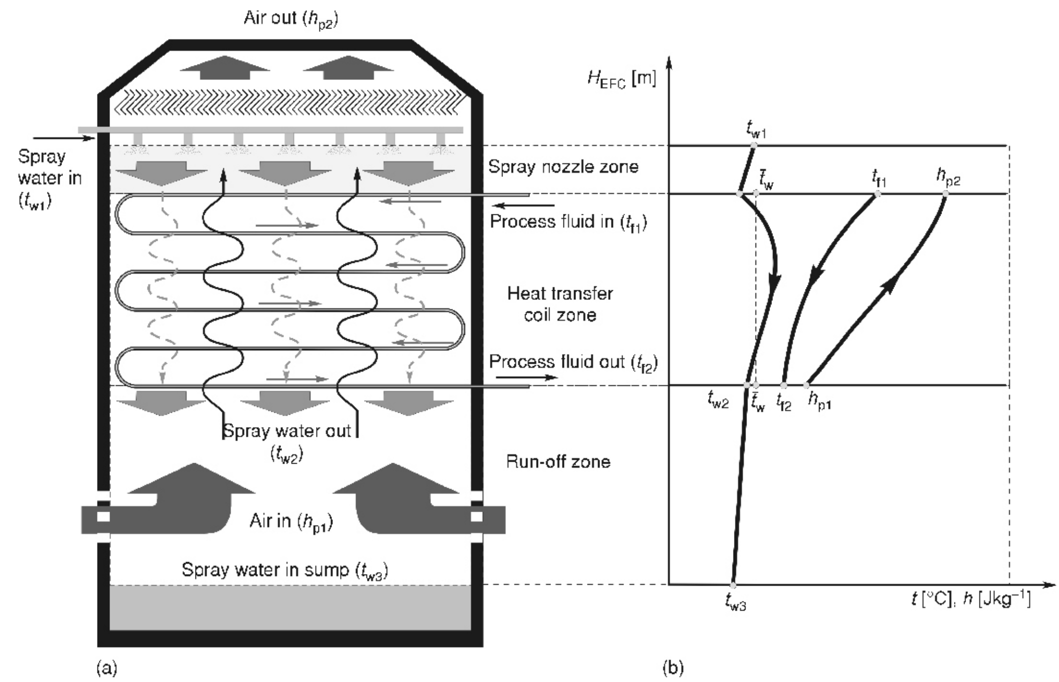

Figure 1. (a) Schematic of the EFC and (b) expected temperature and enthalpy distribution in EFC

External water is pumped (from outside source or from the sump) to the top of the EFC and spread over the top of tube banks via the water distribution system. A part of this water is evaporated into the air while the remainder passes through the tube banks and falls back into the sump. Air from outside entering the unit through the intakes near the base. The air, forced by the fan, travels upward through the EFC, opposing the flow of the falling water. Eliminator plates are positioned near the air outlet to minimize drift or carryover of water droplets in the exhaust air. In closed circuit, process fluid is cooled inside the tubes and does not come into contact with the spray water or the air flowing through the unit. Pure process fluid returns to the system without the formation of deposits and scale, resulting in lower operating costs.

The cooling rate is affected by the two processes. The first, heat carried away from the process, transfers to the spray water film through the tube walls. On that way spray water play a role of an intermediate fluid, since it creates the water film on the outer side of the tubes. The second, heat from water film is transfer to the forced air flow. This transfer is realized in both, sensible and latent forms. The sensible heat is caused by the temperature gradient between the spray water and the air, while the latent heat is produced by the evaporation of a small amount of the spray water into the air stream. The latent heat plays an important role in the transfer processes and greatly enhances the heat transfer. Khan *et al.* [3] demonstrated that evaporation contributes about 62.5% of the total rate of heat transfer at the bottom of the EFC, and almost 90% at the top of the EFC. Figure 1b illustrates the expected trends of spray water temperature and air enthalpy corresponding to elevation above the sump level. In this paper, the constant spray water temperature $\bar{t}_w$ will be taken equal to the inlet spray water temperature t_{w1} measured from the experiments.

Thermal models for evaporative fluid coolers

The thermal analysis of EFC unit is inherently complicated because the cooling process involves simultaneous heat and mass transfer processes. For that reason a lot of different numerical models, classified as detailed or simple (correlation-based), are developed in the past [4].

Detailed models use complex mathematical formulation and require detailed data about the physical characteristics of the equipment (size and arrangement of heat exchanger tubes) and the thermal phenomena (uniformity of the water distribution, cooling capacity and air velocity across the tubes) occurring within the EFC. Detailed models are based on a CFD-type approach, involving the numerical solution of differential equations for air/spray water flow, energy and water vapor concentration. After velocity, temperature and humidity fields are generated; transfer coefficients can be calculated as a result. Although a detailed analysis of air and spray water distribution in the EFC is possible, they have some limitations [5, 6]. These models and codes also consume considerable computing time and require a certain degree of specialization.

The correlation based models use the relationship between the energy performance of the EFC and different operating or construction parameters. Correlation models are based on local energy and mass balances equations and may also need the solution of differential equations, although not necessarily. All correlation based models assume some simplifications, like the tube surface is completely wet or the spray water is uniformly distributed over the tube bundle. This approach is more practical and may also lead to improved accuracy. It has to be said that correlation based models are valid within the range of parameters used in their development, but their extrapolation out of this range have to be done very carefully.

The origin of EFC modeling process can be found in the work of Merkel [7]. In 1925, Merkel proposed a theory relating evaporation and sensible heat transfer in the case of counter flow contact of water and air, such as in cooling tower. Using a number of assumptions and approximations such as negligible water loss due to evaporation, the one-dimensional equations for heat and mass transfer are reduced in a single separate ordinary differential equation. The approximate method developed by Merkel has been used for the design of cooling towers for decades.

In the case of EFC and ECN, first modeling procedure, each with a varying degree of approximation, can be found in the literature [8-10]. Most of the models given in the literature [4, 11, 12] prior to 1960 were derived by assuming a constant or a theoretically constant spray water temperature [13] and were still utilized in some recent studies for interpretation of experimental data for getting the relevant heat and mass transfer coefficients [13-15].

Later, thermal performance was subjected to mathematical and experimental analysis in the work of Parker *et al.* [16], Mizushina *et al*. [17, 18], and Niitsu *et al.* [19]. Parker *et al.* [16] presented an analytical method in which they consider the temperature variation of spray water along the tubes. The solution of the governing differential equations was achieved by assuming a linear relation between the spray water temperature and enthalpy of the saturated air-water mixture. In the same reference, they also reported a detailed experimental study to define the heat and mass transfer characteristics of evaporative fluid coolers. The development of Parker *et al*. is followed by Leidenfrost *et al*. [20], who demonstrated that the numerical solutions for proper design can only be obtained by iterative techniques. They presented a graphical procedure which was executed by a computer program in a stepwise integration.

Mizushina *et al*. (1967) [17] presented two methods of heat calculation in coolers: one simplified, with constant spray water temperature and another, which took into account the variation of that temperature. They applied the assumption of constant spray water temperature to evaluate the empirical heat and mass transfer correlations. The mass transfer coefficient were presented in terms of the air and spray water Reynolds numbers. In the next paper [18] they developed two different rating methods for EFC.

Zalewski [1] and Zalewski *et al.* [2] presented a mathematical model of EFC, based on the heat and mass transfer equations for non-adiabatic evaporation. The mass transfer coefficient is obtained by analogy with heat transfer correlations of fluid flow across tube bundles. A correction for the mass transfer coefficient was suggested as a function of inlet air wet bulb temperature. On that way, the agreement between calculated data and experimental results are improved.

In comprehensive review Ren *et al.* [11] concluded that heat and mass transfer processes in different EFC regime (wet or dry) are similar and can be described with the same set of differential equations. The differences are in their heat and mass transfer coefficients and heat capacities of the fluid streams for different regimes. Authors proposed analytic methods which apply incomplete surface wetting condition. Also they took in consideration the effects of spray water evaporation, temperature variation, and enthalpy change along the heat exchanger surface in order to get more accurate results.

The mathematical model which will be presented in this paper is similar to the correlation based model developed by Zalewski [1] and Zalewski *et al.* [2]. Numerical integration of model is executed by application of differential, collocation Simpson method and the results of calculation are compared with the results obtained from the experimental measurements. For that reason the paper comprise a description of experimental installation, modeling and numerical procedure, followed by the error analysis of results.

Experimental system

Schematic diagram of experimental installation, followed by photographs, is presented in fig. 2. Evaporative heat exchanger consists of square arranged tube bundle, made by 13 pipes (15/13 mm) in 10 passes which are connected with collectors. Horizontal distance between pipes is 36 mm, and vertical pitch is 60 mm. The casing (470   470 mm) is partly made of acrylic sheet of 10 mm thickness so that the flow of water inside the tower can be clearly viewed from outside. Process fluid (hot water) is pumped from the storage tank which is heated by heaters and controlled by temperature controller. Spray jet of the cooling water, obtained from the local water supply, is spreading over the tube bundle and collecting into the sump. Their flow rates are adjusted by flow control valves (TA-STAD throtling valve) and CBI acquisition system. Moist air, enters from bottom, flow in the upward direction countering the flow of the spray water, and is finally discharged to the atmosphere. Forced air flow is provided by centrifugal fan, while water drops removal is prevented by the droplet eliminator. Humidity ratio and dry bulb temperature are measured via hygrometer (psychrometer) in which its measuring tip is protected from contacting water. Air flow rate is determined by TESTO 454 measuring system.

During the research 27 experiments are accomplish. According to the inlet temperature of process fluid procedures are divided in three groups: regime t_{f1} = 37 °C, regime t_{f1} = = 47 °C, and regime t_{f1} = 57 °C. The other experimental condition as well the results obtained by measurments are presented in Apendix.

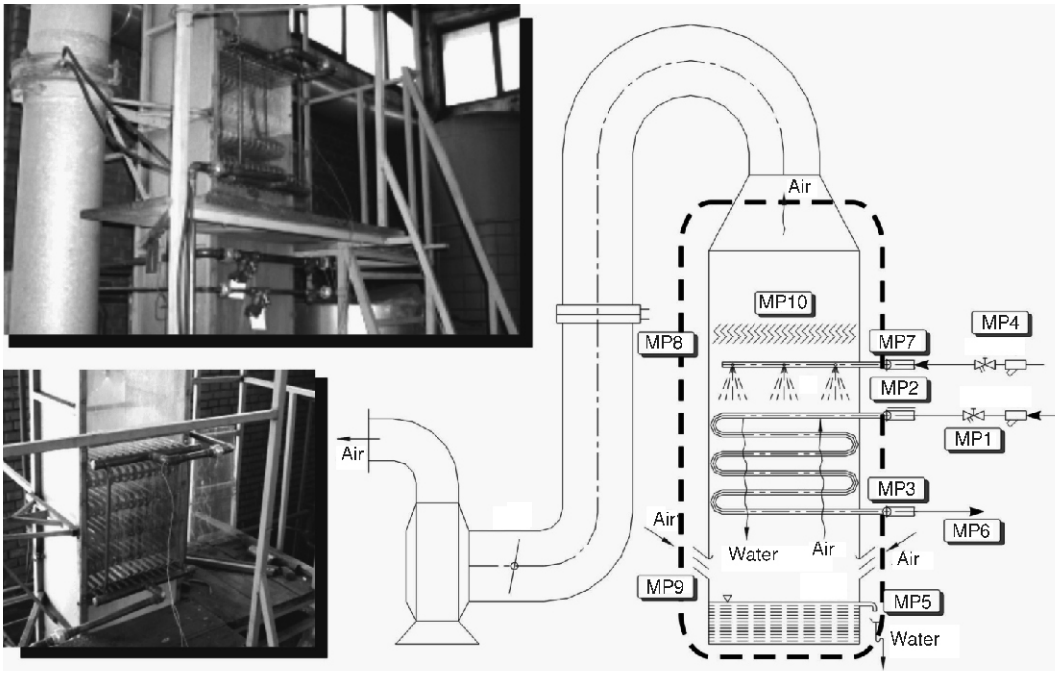

Figure 2. Schematic diagram of experimental system

Mathematical model of the process in EFC

The mass and energy balance equations, that form the mathematical model of EFC, are derived from the infinitesimal element of surface area presented in fig. 3. In this element the air (subsystem I) is flowing in upward direction whereas the spray water (subsystem II) and process fluid (subsystem III) flows is downward direction (fig. 4), which is also a positive direction of the variable l.

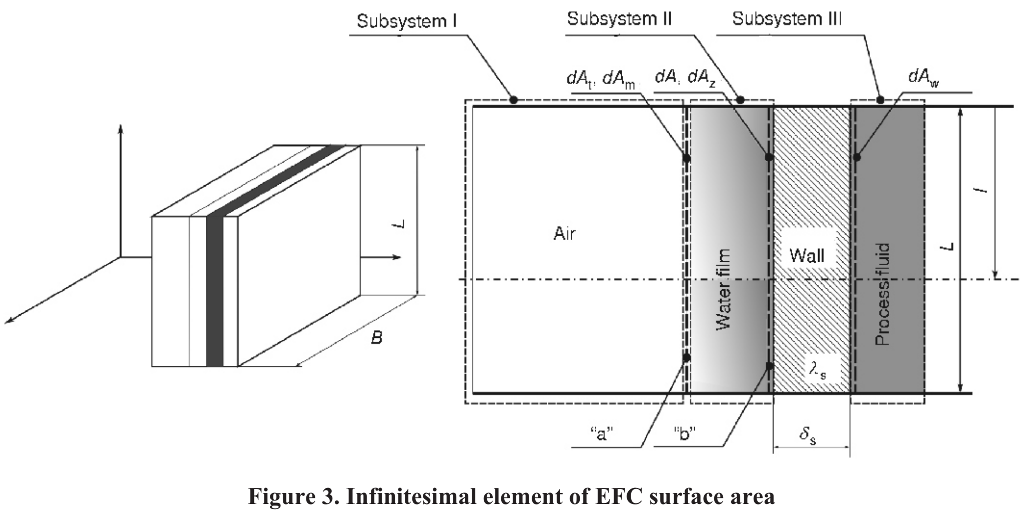

Figure 3. Infinitesimal element of EFC surface area

The major assumptions involved in modeling may be summarized as [2, 11, 21, 22]:

– the system is in a steady-state,
– no heat transfer to the surroundings occurs, and radiation heat transfer is ignored,
– specific heat capacities, as well the heat and mass transfer coefficients are constant,
– fluids at entry are uniformly distributed in the plane perpendicular to the flow,
– mass and heat transfers take place only in the direction normal to the flow,
– complete surface wetting of the tube bundle is assumed, and
– resistance of the heat transfer from the water layer core to its surface is neglected; a temperature of the water at an inter phase surface is equal to an average value; according to [23] the temperature difference, in this case, does not exceed 0,4%.

Balance equations for subsystem limited by controlled volume "a" (subsystem I):

Mass balance equation:

$$\mathrm{d}\dot{m}_{\mathrm{w}} \quad \mathrm{d}\dot{W} \tag{1}$$

where

$\mathrm{d}\dot{W} \quad \beta_{\mathrm{x}}[x \ (t_{\mathrm{w}}) \quad x]\mathrm{d}A_{\mathrm{m}}$ – mass flux of water which evaporates into air,

$x \quad \dfrac{0.622 p_{\mathrm{pw}}}{p \quad p_{\mathrm{pw}}}$ and $x \quad \dfrac{0.622 p_{\mathrm{pw}}}{p \quad p_{\mathrm{pw}}}$ – humidity ratio for saturated and non-saturated air,

$p_{pw} \quad p_{\mathrm{pw}}(t_{\mathrm{b}}) \quad \dfrac{0.5}{755} p(t_{\mathrm{p}} \quad t_{\mathrm{b}})$ – partial pressure of water vapor in air,

$p_{\mathrm{pw}}(t) \quad p_0 \quad 10^V$ – partial pressure of water vapor at a saturation state,

$V \quad \dfrac{t}{31.6639 \quad 0.131305t \quad 2.63247 \quad 10 \quad ^5 t^2}$ – values of the coefficients (from 0 to 100 °C), and

$\mathrm{d}A_{\mathrm{m}} = a_{\mathrm{m}}\mathrm{d}A = a_{\mathrm{m}}B\mathrm{d}l$ – infinitesimal surface area (mass transfer from water to air).

Energy balance equation:

$$\dot{m}_{\mathrm{ps}}\mathrm{d}h_{\mathrm{p}} \quad \mathrm{d}\dot{W}h_{\mathrm{pw}} \quad \delta\dot{Q}_{\mathrm{p}} \tag{2}$$

where

$h_{\mathrm{p}} = c_{\mathrm{ps}}t_{\mathrm{p}} + x(c_{\mathrm{pw}}t_{\mathrm{p}} + 2500.8)$ – specific enthalpy of moist air,

$h_{\mathrm{pw}} = c_{\mathrm{pw}}t_{\mathrm{w}} + 2500.8$ – specific enthalpy of water vapor,

$\delta\dot{Q}_{\mathrm{p}} \quad \alpha_{\mathrm{p}}(t_{\mathrm{w}} \quad t_{\mathrm{p}})\mathrm{d}A_{\mathrm{t}}$ – heat flux from the water surface to the humid air, and

$\mathrm{d}A_{\mathrm{t}} = a_{\mathrm{t}}\mathrm{d}A = a_{\mathrm{t}}B\mathrm{d}l$ – infinitesimal surface area of heat transfer from water to air.

Balance equations for subsystem limited by controlled volume "b" (subsystem I + II)

Mass balance equation:

$$\mathrm{d}\dot{m}_{\mathrm{w}} \quad \dot{m}_{\mathrm{ps}}\mathrm{d}x \tag{3}$$

Energy balance equation:

$$\dot{m}_{\mathrm{ps}}\mathrm{d}h_{\mathrm{p}} \quad \delta\dot{Q}_{\mathrm{k}} \quad \dot{m}_{\mathrm{w}}\mathrm{d}h_{\mathrm{w}} \quad h_{\mathrm{w}}\mathrm{d}\dot{m}_{\mathrm{w}} \tag{4}$$

where

$h_\mathrm{w} = c_\mathrm{w} t_\mathrm{w}$ – specific enthalpy of water,

$\delta \dot{Q}_\mathrm{k} \quad k_\mathrm{z}(t_\mathrm{f} \quad t_\mathrm{w})\mathrm{d}A_\mathrm{s}$ – heat flux from process fluid to the water film,

$\mathrm{d}A_\mathrm{s} = a_\mathrm{s}\mathrm{d}A$ – infinitesimal surface area of heat conduction through the wall, and

$$k_\mathrm{z} \quad \frac{1}{\dfrac{1}{\alpha_\mathrm{f}}\dfrac{A_\mathrm{z}}{A_\mathrm{w}} \quad \dfrac{\delta_\mathrm{s}}{\lambda_\mathrm{s}}\dfrac{A_\mathrm{z}}{A_\mathrm{s}} \quad \dfrac{1}{\alpha_\mathrm{w}}}$$

– overall heat transfer coefficient.

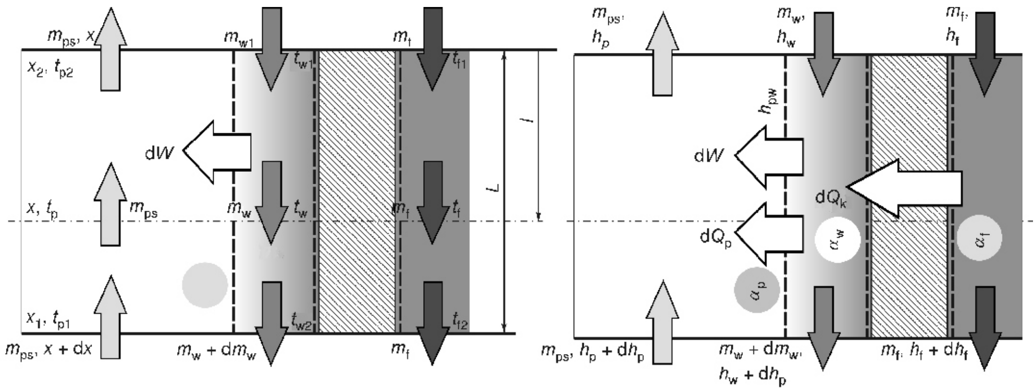

Figure 4. Process diagram for an infinitesimal element of surface area

Balance equations for process fluid subsystem, (subsystem III)

Energy balance:

$$\delta \dot{Q}_\mathrm{k} \qquad \dot{m}_\mathrm{f}\mathrm{d}h_\mathrm{f} \qquad \dot{m}_\mathrm{f} c_\mathrm{f}\mathrm{d}t_\mathrm{f} \tag{5}$$

By a suitable rearrangement of above balance equation the set of four ordinary differential equations is obtained. This system of the eqs. (6-9) presents a mathematical model of the considered process for counter current flow of cooling water and the air:

$$\frac{\mathrm{d}x}{\mathrm{d}l} \qquad \frac{\beta_\mathrm{x} a_\mathrm{m} B[x \;\, (t_\mathrm{w}) \quad x]}{\dot{m}_\mathrm{ps}} \tag{6}$$

$$\frac{\mathrm{d}t_\mathrm{p}}{\mathrm{d}l} \qquad \frac{B(t_\mathrm{w} \quad t_\mathrm{p})}{\dot{m}_\mathrm{sv} c_\mathrm{v}}\{\beta_\mathrm{x} a_\mathrm{m} c_\mathrm{pw}[x \;\, (t_\mathrm{w}) \quad x] \quad a_\mathrm{t}\alpha_\mathrm{p}\} \tag{7}$$

$$\frac{\mathrm{d}t_\mathrm{w}}{\mathrm{d}l} \qquad \frac{B}{\dot{m}_\mathrm{w} c_\mathrm{w}}\{\beta_\mathrm{x} a_\mathrm{m}[t_\mathrm{w}(c_\mathrm{w} \quad c_\mathrm{pw}) \quad r_0][x \;\, (t_\mathrm{w}) \quad x] \quad \alpha_\mathrm{p} a_\mathrm{t}(t_\mathrm{w} \quad t_\mathrm{p}) \quad k_\mathrm{z}(t_\mathrm{f} \quad t_\mathrm{w})\} \tag{8}$$

$$\frac{\mathrm{d}t_\mathrm{f}}{\mathrm{d}l} \qquad \frac{k_\mathrm{z}(t_\mathrm{f} \quad t_\mathrm{w})}{\dot{m}_\mathrm{f} c_\mathrm{f}} \tag{9}$$

where

$\dot{m}_\mathrm{w} \quad \dot{m}_\mathrm{w\,in} \quad \dot{m}_\mathrm{ps}(x_2 \quad x)$ – water mass flow through an arbitrary cross-section,

$c_\mathrm{p} = c_\mathrm{ps} + xc_\mathrm{pw}$ – specific heat of moist air, and

$x(\mathrm{L}) = x_1$, $t_\mathrm{p}(\mathrm{L}) = t_{\mathrm{p}1}$, $t_\mathrm{w}(0) = t_\mathrm{w}(\mathrm{L})$, $t_\mathrm{f}(0) = t_{\mathrm{f}1}$ – boundary conditions for the system equations.

Introduced equations can be translated in a dimensionless form, by the use of dimensionless variables presented in tab. 1. This operation is followed by new boundary conditions and redefinition of some values.

Table 1. Dimensionless variables and new boundary conditions

Variables	Dimensionless variables	Boundary conditions
Height	$l^* \quad \dfrac{l}{L}$	
Air temperature	$t_\mathrm{p}^* \quad \dfrac{t_\mathrm{p}}{t_\mathrm{p}(l \quad L) \quad t_{\mathrm{p}1}}$	$t_\mathrm{p}^*(l^* \quad 1) \quad 1$
Humidity ratio	$x^* \quad \dfrac{x}{x(l \quad L) \quad x_1}$	$x^*(l^* \quad 1) \quad 1$
Cooling water temperature	$t_\mathrm{w}^* \quad \dfrac{t_\mathrm{w}}{t_\mathrm{p}(l \quad L) \quad t_{\mathrm{p}1}}$	$t_w^*(l^* \quad 1) \quad t_w^*(l^* \quad 0)$
Operating fluid temperature	$t_\mathrm{f}^* \quad \dfrac{t_\mathrm{f}}{t_\mathrm{f}(l \quad L) \quad t_{\mathrm{p}1}}$	$t_\mathrm{f}^*(l^* \quad 0) \quad 1$
Humidity ratio for saturated air	$(x \ )^* \quad x \ (t_\mathrm{w}^*) \quad \dfrac{\dfrac{0.622}{x_1} p_\mathrm{p}(t_\mathrm{w}^*)}{p \quad p_\mathrm{p}(t_\mathrm{w}^*)}$	
Specific heat of moist air	$c_\mathrm{p} \quad c_\mathrm{p}(x^*) \quad c_{sv} \quad c_{\mathrm{pw}} x_1 x^*$	
The partial pressure of water vapour in air	$p_\mathrm{p}(t_\mathrm{w}^*) \quad p_0 \; 10^V, \quad V \quad \dfrac{t_\mathrm{w}^*}{\dfrac{31.6639}{t_{\mathrm{p}1}} \quad 0.131305 t_\mathrm{w}^* \quad 2.63247 \; 10^{\ 5} t_{\mathrm{p}1}(t_\mathrm{w}^*)^2}$	

* In a case of spray water flow in open circuit: $t_\mathrm{w}^*(l^* \quad 0) \quad t_{\mathrm{w}1}/t_{\mathrm{p}1}$

By using the rules of a complex function derivation and definitions of dimensionless values, the system of the eqs. (6)-(9) obtained the following forms:

$$\frac{\mathrm{d}x^*}{\mathrm{d}l^*} \quad R_\mathrm{x}[(x \ )^* \quad x^*] \tag{10}$$

$$\frac{\mathrm{d}t_\mathrm{p}^*}{\mathrm{d}l^*} \quad R_\mathrm{p}(t_\mathrm{w}^* \quad t_\mathrm{v}^*)\{x_1[(x \ )^* \quad x^*] \quad R_1\} \tag{11}$$

$$\frac{\mathrm{d}t_\mathrm{w}^*}{\mathrm{d}l^*} \quad \frac{R_\mathrm{w}}{\dfrac{\dot{m}_{\mathrm{w}1}}{\dot{m}_\mathrm{ps}} \quad x_1(x_2^* \quad x^*)}$$

$$\frac{R_\mathrm{x}}{R_\mathrm{w}} \quad 1 \; t_\mathrm{w}^* \quad R_\mathrm{pw} \; [(x \ )^* \quad x^*]x_1 \quad R_1(t_\mathrm{w}^* \quad t_\mathrm{p}^*) \quad R_\mathrm{k} \; t_\mathrm{f}^* \frac{t_{\mathrm{f}1}}{t_{\mathrm{p}1}} \quad t_\mathrm{w}^* \tag{12}$$

$$\frac{\mathrm{d}t_\mathrm{f}^*}{\mathrm{d}l^*} \quad R \;\; t_\mathrm{f}^* \quad \frac{t_{\mathrm{p}1}}{t_{\mathrm{f}1}} t_\mathrm{w}^* \tag{13}$$

Dimensionless numbers which appear in these equations are defined as:

$$R_{\mathrm{x}} \quad \frac{a\beta_{\mathrm{x}}BL}{\dot{m}_{\mathrm{ps}}}; \quad R_{l} \quad \frac{\alpha_{\mathrm{p}}}{\beta_{\mathrm{x}}c_{\mathrm{pw}}}; \quad R_{\mathrm{p}} \quad R_{\mathrm{x}}\frac{c_{\mathrm{pw}}}{c_{\mathrm{p}}}; \quad R_{\mathrm{w}} \quad R_{\mathrm{x}}\frac{c_{\mathrm{pw}}}{c_{\mathrm{w}}};$$

$$R_{\mathrm{p}} \quad \frac{r_0}{c_{\mathrm{pw}}t_{\mathrm{pl}}}; \quad R_{\mathrm{k}} \quad \frac{k_{\mathrm{z}}}{a\beta_{\mathrm{x}}c_{\mathrm{p}}}; \quad R_{\mathrm{f}} \quad \frac{k_{\mathrm{z}}LB}{\dot{m}_{\mathrm{f}}c_{\mathrm{f}}}$$

In order to adapt the mathematical model of heat and mass transfer to the geometry of bare-tube exchanger, the volume of exchanger is divided in to elements [1] which mutual influence may be neglected. These elements present separate heat exchangers, which number is equal to the number of coils. Exchanger heat performance is equal to the sum of heat performances of all elements. In each element, water down-flow across the tubes, is presented as flow down two vertical surfaces (to each of them is assigned half of the mass flux of process fluid in the tubes). The height of the exchanger, which is also the interval of integration of eqs. (10-13), is determined as the sum of half-perimeters in all coil tubes. Assuming the equality of surface for heat and mass transfer, the area ratios are calculated as $a_{\mathrm{t}} = a_{\mathrm{m}} = a$.

Numerical solution procedure

The system of the eqs. (10)-(13) together with boundary conditions and the accompanying algebraic equations for dimensionless numbers makes a mathematical model of processes which occur in EFC. In order to obtained the numerical solution of this model it was required to determine the values of heat transfer coefficients (α_{f}, α_{w}, and α_{v}) as well as the coefficient of mass transfer β_{x}.These coefficients are calculated from simplified empirical relations presented in tab. 2.

Table 2. Empirical relation for calculation of heat and mass transfer coefficients

Coefficient	Empirical relation	Range/value
Heat transfer from process fluid inside the tubes [24]	$\mathrm{Nu}_{\mathrm{f}} \quad \dfrac{\frac{\xi_{\mathrm{t}}}{8}(\mathrm{Re}_{\mathrm{f}} \quad 1000)\mathrm{Pr}_{\mathrm{f}}}{1 \quad 12.7\sqrt{\frac{\xi_{\mathrm{t}}}{8}}(\mathrm{Pr}_{\mathrm{f}}^{2/3} \quad 1)} \quad 1 \quad \dfrac{d_{\mathrm{in}}}{L_{\mathrm{r}}}^{2/3}$	
Heat transfer between water and the horizontal tubes [25]	$\mathrm{Nu} \quad 3.3 \; 10 \;^{3}\,\mathrm{Re}^{0.3}\,\mathrm{Re}_{\mathrm{p}}^{0.15}\,\mathrm{Pr}^{0.61}$ $\mathrm{Nu} = 1.1\cdot 10^{-2}\,\mathrm{Re}^{0.3}\,\mathrm{Pr}^{0.62}$ $\mathrm{Nu} \quad 0.24\,\mathrm{Re}^{0.3}\,\mathrm{Re}_{\mathrm{v}}^{0.36}\,\mathrm{Pr}^{0.66}$ $\mathrm{Re}_{\mathrm{p}} \quad \dfrac{w_0 d_z \rho_{\mathrm{p}}}{\mu_{\mathrm{p}}} \quad \mathrm{Re}_w \quad \dfrac{4\Gamma}{\mu_{\mathrm{w}}}$	Re_{p} = 690-3000 Re_{p} = 3000-6900 $\mathrm{Re}_{\mathrm{p}} > 6900$
Heat transfer between the layers of the cooling water and humid air [26]	$\mathrm{Nu}_{\mathrm{w}} \quad n_0 \; \dfrac{S_{\mathrm{q}}}{d_{\mathrm{ex}}}^{n_1} \dfrac{S_1}{d_{\mathrm{ex}}}^{n_2} \dfrac{S_{\mathrm{q}}}{S_1}^{n_3} \; 1 \quad \dfrac{d_{\mathrm{ex}}}{S_{\mathrm{q}}}^{n_4} \; \mathrm{Re}_{\mathrm{w}}^{n_5}\,\mathrm{Pr}_{\mathrm{w}}^{1/3}$ $\mathrm{Nu}_{\mathrm{w}} \quad \dfrac{v_w^2}{\mathrm{g}}^{0.33} \dfrac{\alpha_{\mathrm{w}}}{\lambda_{\mathrm{w}}}$	$n_0 = 0.19086$ $n_1 = 33.490$ $n_2 = -33.328$ $n_3 = -33.508$ $n_4 = -0.14293$ $n_5 = 0.63352$
Mass transfer coefficient β_{x} [27]	$\dfrac{\alpha_{\mathrm{p}}}{\beta_{\mathrm{x}}c_{\mathrm{p}}} \quad \mathrm{Le}^{2/3}$	Le = 0.865

In the phase of numerical integration, proposed mathematical model is presented as system of the first order non linear differential equations with two points boundary conditions. This problem has been resolved by application of differential, collocation Simpson method [28]. The method uses a mesh of points to divide the interval of integration into subintervals. It determines a numerical solution by solving a global system of algebraic equations resulting from the boundary conditions, and the collocation conditions imposed on all the subintervals. If the solution does not satisfy the tolerance criteria, the mesh is adapted and the process is repeated. The method assumes that the points of the initial mesh as well as an initial approximation of the solution at the mesh points are provided.

Results and discusion

The mathematical model and numerical integration, presented in the previous chapters of the paper, was the base for simulation software created on the MATLAB-programming platform. In order to test the validity and accuracy of the software, comparisons between measurements and computed results, was carried out. Using the same input values of air (absolute humidity and temperature) and process fluid (temperature) the numerical and experimental results are presented in figs. 5, 6, and 7.

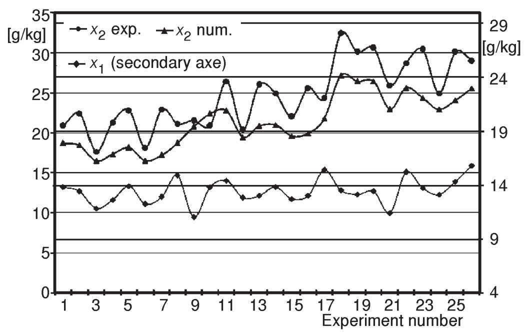

Figure 5. Comparison of computed results with measurements – case absolute humidity

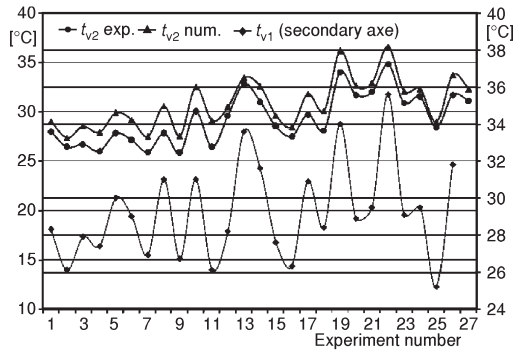

Figure 6. Comparison of computed results with measurement – case air discharge temperature

Error analysis followed by the calculation of average relative error (expressed in percentage) is presented in fig. 8. The figure shows that the computed results are in good agreement with the experimental measurements. The less accuracy in the case of absolute humidity can be explained by the presence of water droplets in the air.

Another comparation was based on heat characteristics of EFC presented in fig. 9. Through comparison, results of numerical integrations were found to be in good agreement with those of experimental mesurments.

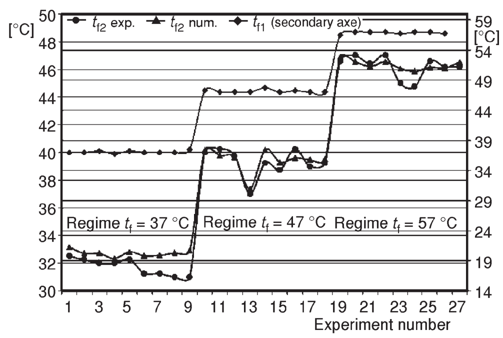

Figure 7. Comparison of computed results with measurements – case process fluid output temperature

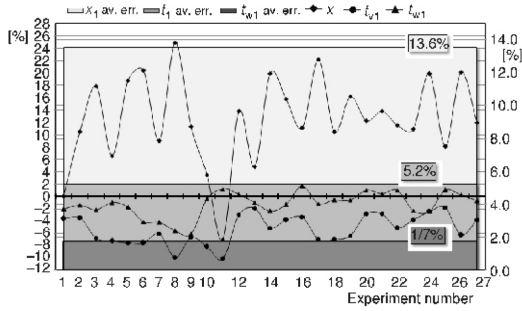

Figure 8. Relative error between computed and experimental results

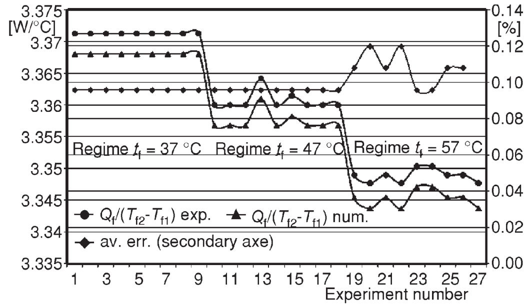

Figure 9. Comparison of computed results with measurements-case heat characteristics of EFC

Conclusions

The phenomenon of cooling by evaporation is promising eco-sustainable technology which can be used in many applications such as power plants, air-conditioning, and refrigeration. In this paper the main objective was thermal analysis through experimental study and numerical analysis of conventional evaporative fluid cooler. Experimental measurements are performed on small scale EFC plant. A numerical analysis has been carried out to explore the detailed heat- and mass-transfer characteristics of this unit. It has been shown that the proposed mathematical model translate in the software for bare-tube EFC design provide the acceptable results in comparing with experimental data.

This part of research enabled the accomplishment of two future goals. First goal is the development of more comprehensive simulation software, with wider range of thermal and construction parameters. Second, advance analysis and improvement of EFC's energy performance based on exergy analysis. The use of exergy concept in evaluating the performance of energy systems are increasing nowadays due to its clear indication of loss at various locations which is more in formative than energy analysis [29].

Nomenclature

A – surface area, [m^2]
a – area ratio, [–]
B – length of heat exchanger, [m]
c – specific heat capacity, [Jkg^{-1}]
d – diameter of tube, [m]
g – acceleration of gravity, [ms^{-2}]
h – specific entalphy, [Jkg^{-1}]
k – overall heat transfer coefficient, [Wm^{-2}K^{-1}]
L – height of heat exchanger, [m]
L_r – length of tube, [m]
Le – Lewis number, [–]
l – length, linear coordinate, [m]
MP – measurement point
$\dot{m}$ – mass flow rate, [kgs^{-1}]
Nu – Nusselt number, [–]
Pr – Prandtl number, [–]
p – presure, [Pa]
Re – Reynolds number, [–]
r – latent heat of vaporization, [Jkg^{-1}]
S – tube spacing, [m]
t – temperature, [°C]
$\dot{W}$ – mass flow rate of water vapour, [kgs^{-1}]
w – flow velocity [ms^{-1}]
x – absolute humidity ratio, [kg$_v$kg$_{sv}$$^{-1}$]

Greek symbols

α – heat transfer coefficient, [Wm^{-2}K^{-1}]
β_x – mass transfer coefficient, [kgm^{-2}s^{-1}]
$\dot{\Gamma}$ – spray density, [kg^{-1}s^{-1}]
λ – thermal condutivity, [Wm^{-1}K^{-1}]
ρ – density, [kgms^{-3}]
φ – relative humidity, [%]

Subscripts and superscripts

1 – inlet value
2 – outlet value
* – dimensionless value
″ – saturation state

ex	– external	ps	– dry air
f	– operational fluid	*s*	– for surface area of heat conduction throught the wall
in	– internal	t	– for surface area of heat transfer from water to air
l	– longitudinal	v	– humid air
m	– for mass transfer from water to air	w	– cooling water
q	– transverse	z	– for wetted surface area
p	– moist air		
pw	– water vapour in air		

References

[1] Zalewski, W., Mathematical Model of Heat and Mass Transfer Processes in Evaporative Condensers, I*nt. J. Refrig., 16* (1993), 1, pp. 23-30

[2] Zalewski, W., Gryglaszewski, P. A., Mathematical Model of Heat and Mass Transfer Processes in Evaporative Coolers, *Chem. Eng. Process., 36* (1997), 4, pp. 271-280

[3] Khan, J. U. R., Yaqub, M., Zubair, S. M., Performance Characteristics of Counter Flow Wet Cooling Towers, *Energy Conversion and Management, 44* (2003), 13, pp. 2073-2091

[4] Facao, J., Oliveira, A.C., Thermal Behavior of Closed Wet Cooling Towers for Use with Chilled Ceilings, *Applied Thermal Engineering, 20* (2000), 13, pp. 1225-1236

[5] Gan, G., Riffat, S. B., Shao, L., Doherty, P., Application of CFD to Closed-Wet Cooling Towers, *Applied Thermal Engineering, 21* (2001), 1, pp. 79-92

[6] Hasan, A., Gan, G., Simplification of Analytical Models and Incorporation with CFD for the Performance Prediction of Closed Wet Cooling Towers, *International Journal of Energy Research, 26* (2002), 13, pp.1161-1174

[7] Merkel, F., Evaporative Cooling, *VDI-Zeitchrift*, 70 (1925), 70, pp. 123-128

[8] Goodman, W., The Evaporative Condenser, *Heat Piping Air Conditioning, 10* (1938), pp. 165-328

[9] Thomsen, E. G., Heat Transfer in an Evaporative Condenser, *Refrigeration Eng., 51* (1946), 5, pp. 425-431

[10] Wile, D. D., Evaporative Condenser Performance Factors, *Refrigeration Eng., 58* (1950), 1, pp. 55-63

[11] Ren, C., Yang, H., An Analytical Model for the Heat and Mass Transfer Processes in Indirect Evaporative Cooling with Parallel/Counter Flow Configurations, *International Journal of Heat and Mass Transfer, 49* (2006), 3-4, pp. 617-627

[12] Jang, J. Y, Wang, Z. G., Heat and Mass Transfer Performance of Closed-Type Towers, Advances in Computational Heat Transfer II, *Proceedings,* Symposium of the International Centre for Heat and Mass Transfer, Queensland, Australia, 2001, pp. 269-276

[13] Erens, P. J, Dreyer, A. A., Modeling of Indirect Evaporative Coolers, *Int. J. Heat Mass Transfer, 36* (1993), 1, pp. 17-26

[14] Hasan, A., Siren, K., Performance Investigation of Plain and Finned Tube Evaporatively Cooled Heat Exchangers, *Appl. Thermal Eng., 23* (2003), 3, pp. 325-340

[15] Hasan, A., Siren, K., Performance Investigation of Plain Circular and Oval Tube Evaporatively Cooled Heat Exchangers, *Appl. Thermal Eng., 24* (2004), 5-6, pp. 779-790

[16] Parker, R. O., Treybal, R. E., The Heat-Mass Transfer Characteristics of Evaporative Coolers, *Chemical Engineering Progress Symposium Series, 57* (1962), 32, pp. 138-149

[17] Mizushina, T., R. Ito, R., Miyashita, H., Experimental Study of an Evaporative Cooler, *International Chemical Engineering, 7* (1967), 4, pp. 727-732

[18] Mizushina, T., R. Ito, R., Miyashita, H., Characteristics and Methods of Thermal Design of Evaporative Cooler, *International Chemical Engineering, 8* (1968), 3, pp. 532-538

[19] Niitsu, Y., Naito, K., Anzai, T., Studies on Characteristics and Design Procedure of Evaporative Coolers, *Journal of SHASE, 43* (1969),7, pp.581-590

[20] Leidenfrost, W., Korenic, B., Evaporative Cooling and Heat Transfer Augmentation Related to Reduced Condenser Temperatures, *Heat Transfer Eng., 3* (1982), 3-4, pp. 38-59

[21] Maclaine-Cross, I. L., Banks, P. J., A General Theory of Wet Surface Heat Exchangers and its Application to Regenerative Cooling, *Journal of Heat Transfer, 103* (1981), 3, pp. 578-585

[22] Kettleborough, C. F., Hsieh, C. S., The Thermal Performance of the Wet Surface Plastic Plate Heat Exchanger Used as an Indirect Evaporative Cooler, *ASME J. Heat Transfer, 105* (1983), pp. 366-373

[23] Zalewski, W., Heat and Fluid Flow Problems in Evaporative Heat Exchangers (in Polish), Monograph 139, Krakow University of Technology, Krakow, Poland, 1992
[24] ***, Heat Exchange by Fluid Flow in Tube (in German) (Ed. V. Gnielinski), VDI-Heating Handbook, VDI-Edition, Düsseldorf, Germany, 1985
[25] Tovaras, N. V., Bykov, A. V., Gogolin, V. A., Heat Exchange at Film Water Flow under Operating Conditions of Evaporative Condenser (in Russian), *Holod Teh,* (1984), 1, pp. 25-29
[26] Grimson, E. D., Correlation and Utilization of New Data on Flow Resistance and Heat Transfer for Cross Flow of Gases Over Tube Banks, *Trans. ASME, 59* (1937), pp. 583-594
[27] Bošnjaković, F., Technical Thermodynamics II (in German), Edition Th. Steinkopff, Dresden and Leipzig, 1965
[28] Ascher, U. M., Mattheij, R. M. R., Russell, R. D. R., Numerical Solution of Boundary Value Problems for Ordinary Differential Equations, Prentice Hall, Upper Saddle River, N. J., USA, 1988
[29] Saravanan, M., Saravanan, R., Renganarayanan, S., Energy and Exergy Analysis of Counter Flow Wet Cooling Tower, *Thermal Science, 12* (2008), 2, pp. 69-78

Apendix: Experimental conditions and results of measurements

	Process fluid			Spray water		Water in sump		Loss	Air						
	MP1 m_f [kg/s]	MP2 t_{f1} [°C]	MP3 t_{f2} [°C]	MP4 m_{w1} [kg/s]	MP7 t_{w1} [°C]	MP5 m_{w2} [kg/s]	MP5 t_{w2} [°C]	MP6 m_{wz} [kg/s]	MP8 m_p [kg/s]	MP9 t_{p1} [°C]	MP9 φ_{p1} [%]	MP9 x_{p1} [g/kg]	MP10 t_{p2} [°C]	MP10 φ_{p2} [%]	MP10 x_{p2} [g/kg]
Regime t_{f1} = 37 °C	0.81	37.00	32.50	0.06	15.0	0.02	26.5	0.01	0.78	28.3	49.6	13.70	28.0	80.1	20.6
	0.81	37.00	32.25	0.09	15.0	0.03	26.3	0.02	0.80	26.1	66.5	13.8	26.4	96.5	20.9
	0.81	37.25	32.00	0.12	15.0	0.05	27.0	0.03	0.79	27.9	56.1	13.4	26.7	99.6	22.4
	0.81	36.75	32.00	0.06	15.0	0.01	24.0	0.02	1.10	27.4	51.5	11.8	26.0	82.3	17.6
	0.81	37.25	32.25	0.09	15.0	0.02	25.5	0.04	1.10	30.0	48.3	12.6	27.8	89.4	21.3
	0.81	37.00	31.25	0.12	15.0	0.03	25.2	0.05	1.09	29.0	55.1	13.9	27.1	99.9	22.8
	0.81	37.00	31.25	0.06	15.0	0.01	23.0	0.03	1.25	26.9	55.8	12.2	25.9	85.9	18.1
	0.81	37.00	31.00	0.09	15.0	0.02	25.0	0.05	1.25	31.0	45.5	12.9	27.8	96.2	22.9
	0.81	37.50	31.00	0.12	15.0	0.02	25.0	0.06	1.25	26.7	67.4	14.9	25.8	99.9	21.1
Regime II t_{f1} = 47 °C	0.80	47.25	40.00	0.06	15.0	0.02	28.2	0.01	0.79	31.0	39.1	11.0	30.0	79.6	21.5
	0.80	47.00	40.25	0.09	15.0	0.04	29.1	0.02	0.80	26.1	66.5	13.8	26.4	96.5	20.9
	0.80	47.00	39.75	0.12	15.0	0.05	30.0	0.03	0.79	28.2	61.6	14.4	29.6	99.9	26.4
	0.80	43.25	37.00	0.06	15.0	0.01	27.0	0.02	1.09	33.6	36.2	12.8	32.8	62.4	20.4
	0.80	47.75	39.25	0.09	15.0	0.02	28.0	0.04	1.10	31.6	45.2	13.0	31.1	89.9	26.0
	0.80	47.00	38.75	0.12	15.0	0.03	27.8	0.05	1.09	27.6	59.4	13.8	28.5	99.9	24.9
	0.80	47.25	40.25	0.06	15.0	0.01	24.2	0.02	1.24	26.3	59.2	12.7	27.5	94.4	22.0
	0.80	47.00	39.00	0.09	15.0	0.02	25.8	0.04	1.25	30.9	46.2	13.0	29.7	95.6	25.6
	0.80	47.00	39.25	0.12	15.0	0.02	26.0	0.06	1.25	28.4	63.2	15.4	28.1	99.9	24.3

Apendix: Experimental conditions and results of measurements (continuation)

Regime III t_{f1} = 57 °C	0.80	56.50	46.60	0.06	15.0	0.01	32.0	0.01	0.78	34.0	47.9	13.5	34.0	90.4	32.4
	0.80	57.00	47.00	0.09	15.0	0.03	32.0	0.02	0.79	28.9	53.0	13.1	31.7	99.9	30.1
	0.80	57.00	46.40	0.12	15.0	0.04	32.3	0.03	0.79	29.5	51.7	13.4	32.0	99.9	30.6
	0.80	57.00	47.00	0.06	15.0	0.01	29.0	0.02	1.09	35.6	32.0	11.4	34.8	73.2	25.9
	0.80	56.75	45.00	0.09	15.0	0.02	28.5	0.03	1.10	29.1	61.1	15.2	30.9	99.9	28.7
	0.80	57.00	44.75	0.12	15.0	0.02	29.0	0.05	1.10	29.5	52.7	13.7	31.5	99.9	30.4
	0.80	57.00	46.60	0.06	15.0	0.01	25.1	0.02	1.22	25.2	65.9	13.1	28.4	99.9	24.9
	0.80	56.75	46.20	0.09	15.0	0.01	27.0	0.04	1.25	31.8	49.4	14.3	31.7	99.9	30.1
	0.80	58.00	46.20	0.12	15.0	0.02	27.0	0.05	1.25	29.6	61.1	15.8	31.1	99.9	29.0

Authors' affiliations:

P. Rašković
Faculty of Technology, University of Niš
Leskovac, Serbia

G. Vučković (**corresponding author**)
Mechanical Engineering Faculty, University of Niš
14, Aleksandra Medvedeva Str., 18000 Niš, Serbia
E-mail: vucko@masfak.ni.ac.yu

M. Vukić
Mechanical Engineering Faculty, University of Niš
Niš, Serbia

Paper submitted: May 15, 2008
Paper revised: September 4, 2008
Paper accepted: September 5, 2008